Sensors & Actuators: B. Chemical 317 (2020) 128234

Contents lists available at ScienceDirect

Sensors and Actuators B: Chemical

journal homepage: www.elsevier.com/locate/snb

AlGaN/GaN heterostructure based Pt nanonetwork Schottky diode with water-blocking layer

Kwang Hyeon Baik[a], Sunwoo Jung[b], Chu-Young Cho[c], Kyung-Ho Park[c], Fan Ren[d], Stephen. J. Pearton[e], Soohwan Jang[b,*]

[a] School of Materials Science and Engineering, Hongik University, Jochiwon, Sejong, 339-701, Republic of Korea
[b] Department of Chemical Engineering, Dankook University, Yongin, 16890, Republic of Korea
[c] Nanodevices Laboratory, KoreaAdvanced Nano Fab Center, Suwon 16229, Republic of Korea
[d] Department of Chemical Engineering, University of Florida, Gainesville, FL 32611, United States
[e] Department of Materials Science and Engineering, University of Florida, Gainesville, FL 32611, United States

ARTICLE INFO

Keywords:
Hydrogen sensor
GaN
Pt nanostructure
Humidity
PMGI

ABSTRACT

AlGaN/GaN heterostructure-based Pt nanonetwork Schottky metal contact sensors with polydimethylglutarimide (PMGI) encapsulation as a moisture barrier show robust and reliable response to both dry and humid hydrogen exposures, while maintaining excellent hydrogen sensitivity. Due to the large surface area of the Pt nanonetwork, the detection limit was 0.1 ppm of hydrogen at 25 °C. The thermally stable PMGI encapsulated diode exhibited significant current change under 500 ppm humid hydrogen ambient without degradation of the response up to ~300 °C. The hydrogen responsivity of the Pt nanonetwork diode with PMGI water-blocking layer was modelled in the range of 0.1–40000 ppm with a dissociative Langmuir isotherm. The PMGI encapsulated sensor presents an excellent hydrogen selectivity over other gases, including N_2, NO_2, CO, CO_2, CH_4, and O_2 at 25 °C.

1. Introduction

Extensive research has been conducted on the development of hydrogen sensors since the measurement method for airships filled with hydrogen as a lifting gas was invented in 1904 [1,2]. Hydrogen is a colorless, odorless gas, and the lightest molecule, with a very low density of 0.0899 kg/m^3 and a high diffusion coefficient of 0.61 cm^2/s in air [2–4]. Mainly, it is used in hydrodealkylation, hydrocracking, and hydrodesulfurization processes in chemical plants [5]. Also, hydrogen is required in nuclear power plants as a coolant, in spacecraft as a propellant, and in semiconductor fabrication facility as a carrier gas [2,5]. Recently, hydrogen has attracted great interest as an alternative energy source and a viable energy carrier. Large investments in hydrogen have been made for fuel-cell electric vehicles for light-duty fleets and consumer automobiles [6]. Compared to conventional fossil fuels such as gasoline, hydrogen is one of the most promising pollutant emission-free fuels, with large heat of combustion and energy efficiency. However, many safety concerns exist due to its wide flammability range in air, extremely low ignition energy, relatively high flame velocity, and rapid diffusion characteristics [2–6]. Historically, several severe accidents involving hydrogen have occurred; the Hindenburg disaster in New Jersey in 1937, hydrogen release during maintenance in Houston in 1989, rupture of the storage tank in Frankfurt in 1991, and hydrogen explosion of nuclear power plant in Fukushima in 2011 [2,5]. To prevent similar catastrophe, address public concerns, and make efficient usage of a new energy source, the development of highly sensitive, reliable, and robust hydrogen sensors is essential in industrial and automotive applications.

Various types of hydrogen sensors including electrochemical, catalytic, thermal conductivity, optical and semiconductor-based sensors have been developed [4,7]. Among these, the latter are highly sensitive, low-cost, small and mass producible. The GaN-based material system is one of the most suitable for semiconductor-type hydrogen sensors. Due to its superior material properties, such as wide bandgap of 3.4 eV, chemical and mechanical robustness, excellent carrier transport, and radiation hardness, GaN-based gas sensors exhibit high signal-to-noise ratios, as well as reliable and stable operation at high temperature and in harsh radiative environments [8–18]. One of the biggest merits of GaN based semiconductor is the availability of the AlGaN/GaN heterostructure, in which a two dimensional electron gas (2DEG) channel with mobility of more than 1600 cm^2/V·s forms at the interface between AlGaN and GaN due to spontaneous polarization and piezoelectric

* Corresponding author.
E-mail address: jangmountain@dankook.ac.kr (S. Jang).

https://doi.org/10.1016/j.snb.2020.128234
Received 2 September 2019; Received in revised form 9 January 2020; Accepted 30 April 2020
Available online 05 May 2020

effects [13,14,16,9–18]. The electron conductivity of the 2DEG is sensitive to charge changes on the top AlGaN surface. For Schottky diode AlGaN/GaN heterostructure sensors, Pt is used as Schottky metal electrode and catalytic sensing material for hydrogen detection [14,16,9–18]. Hydrogen molecules are decomposed into atomic hydrogen on the Pt surface, which diffuse into the Pt/AlGaN interface. This dissociated hydrogen forms a dipole moment, resulting in a reduction of Schottky barrier height in the diode and increase of the current through the 2DEG channel when a fixed voltage is applied. By monitoring this current, hydrogen gas in an ambient can be detected. The hydrogen responsivity of AlGaN/GaN based Schottky diode sensor with Pt nanostructure as a Schottky metal contact and sensing material is improved by more than two orders of magnitude compared to Pt film Schottky diodes [14]. The Pt nanostructure has larger surface area, offering more catalytic sites for hydrogen molecules to be adsorbed and dissociated.

One of the biggest issues in semiconductor-based hydrogen sensors is the reduction in responsivity in the presence of humidity [9,16–18]. Water molecules block active sites of Pt for the decomposition reaction of hydrogen molecules, leading to significant degradation of the hydrogen sensitivity. This limits the practical application of the AlGaN/GaN Pt Schottky diode sensor, especially for hydrogen fuel-cell vehicles which require stable operation of the sensor in 95% relative humidity [7].

In this study, we demonstrate that polydimethylglutarimide (PMGI) encapsulation of AlGaN/GaN based hydrogen sensor with Pt nanorod networks (nanonetworks) provide an effective way to eliminate this humidity effect in hydrogen sensing. The device with PMGI water-blocking layer shows a robust response to repeatedly cycled exposure of both dry and humid hydrogen up to 300 °C. The encapsulated device with Pt nanonetworks can detect 0.1 ppm hydrogen at 25 °C. In addition, a dissociative Langmuir isotherm model is presented for the response as a function of hydrogen concentration.

2. Experimental

AlGaN/GaN heterostructures were grown on c-plane sapphire substrates by metal organic chemical vapor deposition (MOCVD) [13,14,16–18]. The epi-layer structure consisted of 2.6 μm GaN and 30 nm $Al_{0.3}GaN$, as shown in Fig. 1. This standard AlGaN/GaN heterostructure has sheet resistance of 320 ohm/square, sheet carrier concentration of 9×10^{12} cm^{-2}, and carrier mobility of 1800 cm^2/Vs. The fabrication of the device started with Ohmic contacts of Ti/Al/Ni/Au (200/800/400/800 Å) deposited by electron beam (e-beam) evaporation. The metal stack was annealed at 850 °C for 1 min under N_2 ambient by rapid thermal annealing (RTA). A 200 nm thick Si_3N_4 passivation layer was deposited by plasma enhanced chemical vapor deposition (PECVD). The window for the Pt nanonetwork active layer contact was opened by buffered oxide etchant (BOE) wet etching. The Pt nanonetwork was spin-coated on the Schottky contact area selectively using conventional photolithography.

The Pt nanonetwork was synthesized by a solution phase method at 25 °C [13,14,19]. 20 mM of K_2PtCl_4 was mixed vigorously with equivolumetric 40 mM cetyltrimethylammonium bromide (CTAB) in chloroform. Then, the Pt precursor was reduced into Pt nanonetwork by adding 300 mM $NaBH_4$. The Pt nanonetwork solution was centrifuged and washed with acetone and ethanol to remove supernatants and surfactants several times.

After Pt nanonetwork deposition, Ti/Au contact pads were deposited by e-beam evaporation. For some diodes, 275 nm of PMGI layer was spun-on the fabricated device as a moisture barrier, and some of this PMGI layer on the contact pad area was removed for electrical probing [17]. Before the PMGI spin-coating, (3-Aminopropyl)triethoxysilane (APTES) was spin-coated to promote the filling of PMGI into the voids in the Pt nanonetwork. The PMGI solution (SF13) was purchased from Microchem, and was composed of the base polydimethylglutarimide with cyclopentanone (65–85 %) and tetrahydrofurfuryl alcohol (10–15 %). Fig. 1 shows a microscopic top-view image and a cross-sectional schematic image of the fabricated Pt nanonetwork sensor with PMGI water-blocking layer. Current-voltage (I–V) characteristics of both the bare and PMGI-coated Schottky diodes were measured at 25–300 °C using an Agilent 4156C parameter analyzer with the diodes in a gas test chamber in ambient of 0.1–40,000 ppm dry hydrogen in air or the same concentrations of hydrogen bubbled through water to produce 99 % relative humidity.

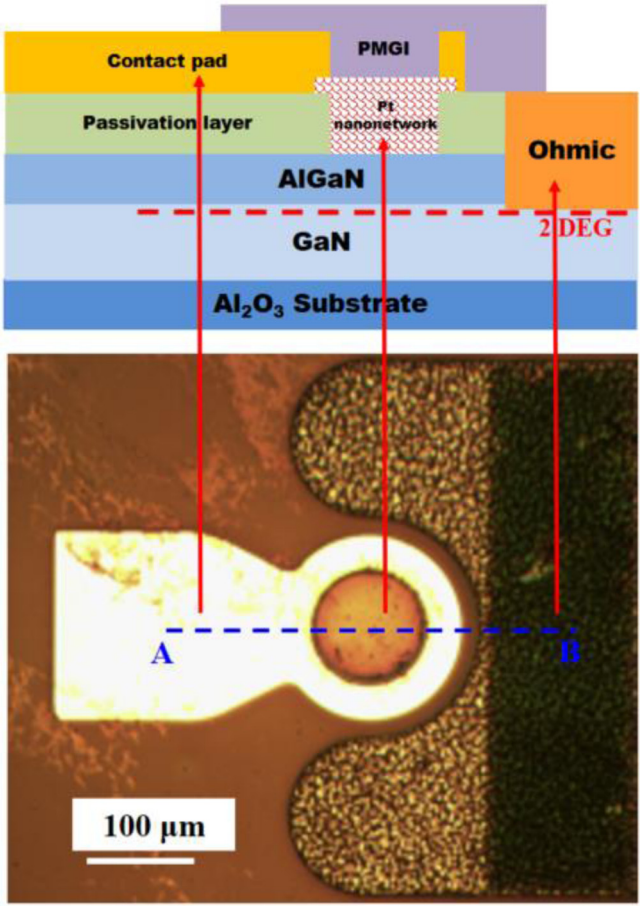

Fig. 1. Cross-sectional schematic image along the cutline of A–B and microscopic image of PMGI encapsulated AlGaN/GaN heterostructure diode with Pt nanonetwork Schottky metal.

3. Results and discussion

Pt nanonetworks with diameter of 2–4 nm were achieved by a simple solution method at 25 °C, as shown in Fig. 2 (a). These Pt nanorods were physically and electrically connected to each other [13,14]. The density of the Pt nanonetwork was controlled by the number of spin-coatings, with 40 times spin-coating performed for our device fabrication. The surface area to unit mass of the Pt nanonetwork is as high as 53 m^2/g, and this large surface area offers more active sites for hydrogen molecules to be adsorbed and decomposed, inducing large current change in the sensor [19]. For conformal encapsulation of the PMGI moisture barrier on the Pt nanonetwork, APTES treatment was employed before PMGI coating. APTES has both polar amine group and nonpolar methyl groups. The amine group is affinitive to the Pt nanonetwork and the methyl group is attracted to the PMGI polymer relatively, hence the APTES surfactant helps to fill out small voids between Pt nanorods with the PMGI. Fig. 2(b) and (c) show scanning electron microscopy (SEM) images of the Pt nanonetwork after 5 h baking on the

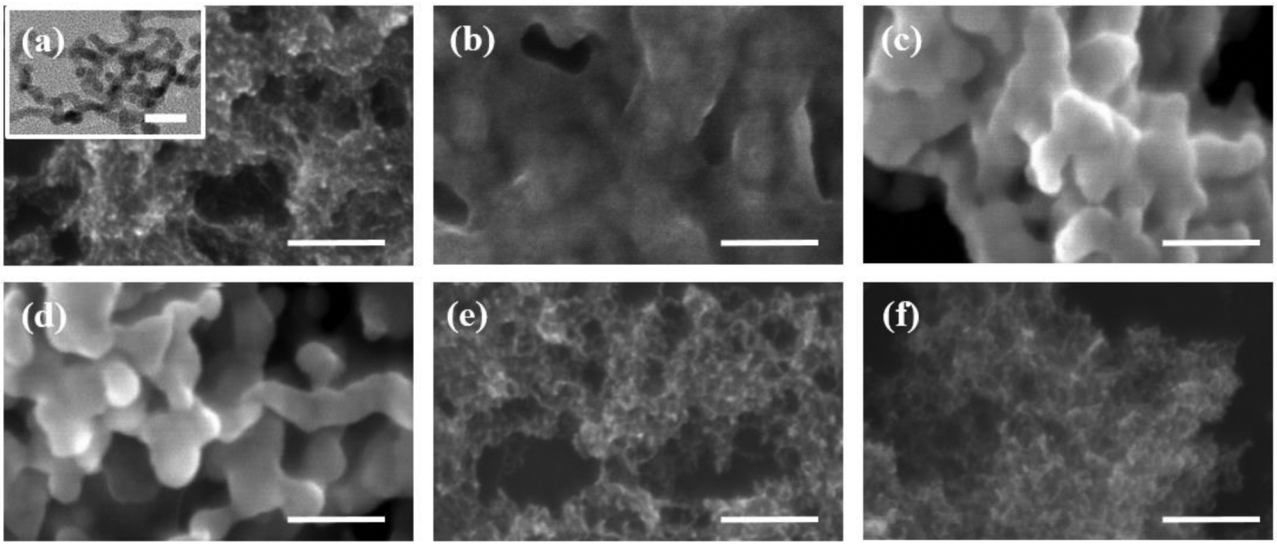

Fig. 2. SEM images of Pt nanonetworks (a) at 25 °C, (b) after 5 h baking at 200 °C without PMGI encapsulation, (c) after 5 h baking at 300 °C without PMGI encapsulation, (d) after 5 h baking at 300 °C without APTES treatment and with PMGI encapsulation, (e) after 5 h baking at 200 °C with APTES treatment and PMGI encapsulation, and (f) after 5 h baking at 300 °C with APTES treatment and PMGI encapsulation. The inset in (a) is the TEM image of Pt nanonetwork as-grown. The scale of the bars in (a), (b), (c), (d), (e), and (f) is 60 nm, and that of the inset in (a) is 10 nm.

hotplate at 200 °C and 300 °C, respectively. Even though the melting point of bulk platinum is 1768 °C, Pt nanorods started to agglomerate together at 200 °C. At 300 °C, Pt nanonetworks with 2–3 nm diameter coalesced into 20–30 nm size Pt clusters, of which surface area is reduced significantly compared to the Pt nanonetwork. Generally, the melting point of Pt nanostructures drops dramatically as the size decreases [20]. The SEM image of Pt nanonetwork with PMGI encapsulation, but without APTES treatment after 5 h baking at 300 °C, is shown in Fig. 2 (d). Agglomerated Pt clusters similar to the case of bare Pt nanonetworks baked at 300 °C were observed, which emphasizes the important role of APTES for conformal filling of Pt nanonetwork with PMGI. In the case of APTES treatment and PMGI encapsulation, the shape of the Pt nanonetwork was maintained up to 300 °C, as seen in Fig. 2 (e) and (f). The effect of the PMGI layer as a water-blocking layer will be discussed later, but the PMGI polymer also works as a supporting filler for the Pt nanonetwork to keep the large surface area at high temperature.

Fig. 3 shows I–V characteristics of PMGI uncoated and encapsulated Pt nanonetwork diodes before and after 500 ppm hydrogen exposure at 25 °C. Under hydrogen ambient, hydrogen molecules penetrate the thin PMGI layer of the PMGI coated device and are adsorbed on the Pt surface. For both bare and encapsulated devices, hydrogen molecules on the catalytic Pt nanonetwork surface are dissociated into atoms, diffuse to AlGaN surface, and form dipoles [13,14,17]. This leads to reduction of Schottky barrier height, resulting in decrease of the turn-on voltage, as well as increase of the diode current. This results in an increase of diode current after 500 ppm hydrogen exposure for both devices. The forward current level of the uncoated diode is higher than the encapsulated device, while the turn-on voltages of both sensors are same regardless of hydrogen exposure. The current level difference is attributed to the difference in contact area between the Pt nanonetwork and AlGaN. Pt nanonetwork was spin-coated on the AlGaN surface randomly, thus the Pt nanonetwork Schottky contact area could not be exactly same for both diodes.

Fig. 4 shows the time-dependent current response of the bare and PMGI coated diodes for 500 ppm hydrogen exposures at 25 °C. The forward bias voltages were 0.6 and 1.4 V at the maximum responsivities obtained for unencapsulated and encapsulated diodes, respectively. A sequence of 500 ppm dry hydrogen, humid hydrogen, and dry hydrogen exposures were cycled into the test chamber, and the chamber was purged with dry air between the cycles. Notably, the unencapulated sensor exhibited a decrease of approximately one twentieth of the

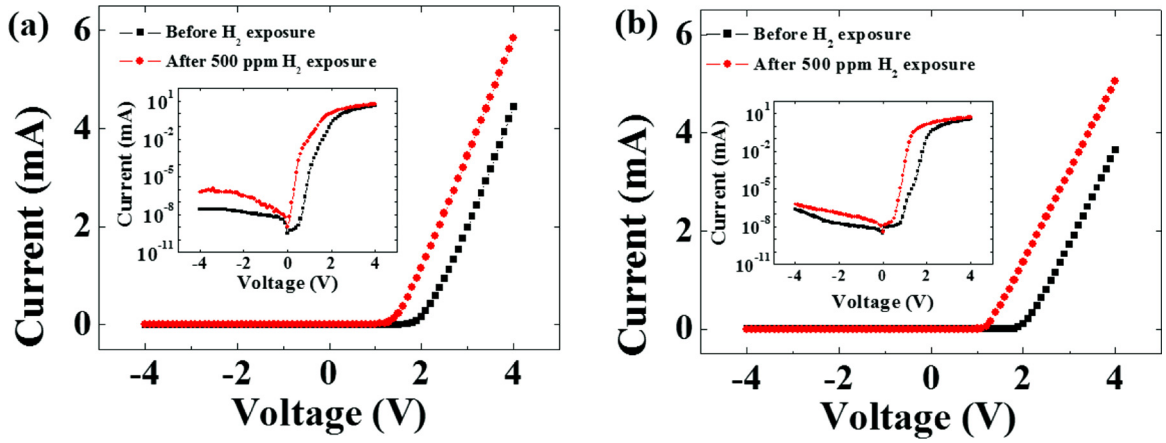

Fig. 3. Forward and reverse current-voltage characteristics of Pt nanonetwork Schottky diode on AlGaN/GaN substrate (a) with PMGI and (b) without PMGI encapsulation before and after dry 500 ppm H_2 in air exposure at 25 °C. The inset shows the same data in a semi-log scale.

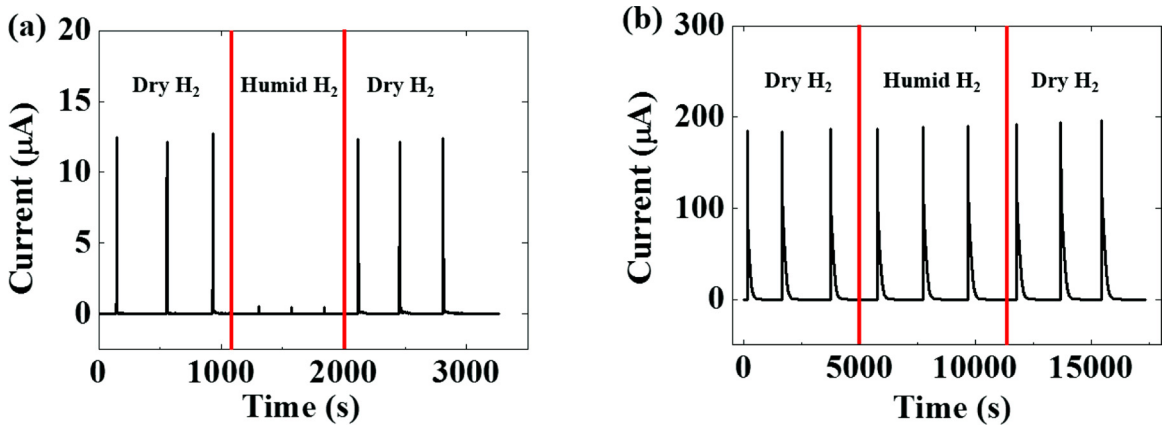

Fig. 4. Time dependence of current change of (a) unencapsulated diode at 0.6 V and (b) PMGI encapsulated sensor at 1.4 V as a function of cyclic ambient of 500 ppm dry, humid, and dry H_2.

current change for detection of 500 ppm humid hydrogen compared to dry hydrogen. In a humid ambient, water molecules block catalytic sites on the Pt surface for adsorption and decomposition of hydrogen, which leads to significant current response drop of the sensor [16–18]. On the contrary, the PMGI encapsulated sensor showed identical current change for both dry and wet 500 ppm hydrogen exposures, as shown in Fig. 4(b). The thin PMGI polymer layer has low moisture permeability and high hydrophobicity [17,21]. The contact angles of Pt film and PMGI film for water were 8° and 71° respectively. Therefore, the PMGI encapsulation layer on the Pt nanonetwork Schottky electrode effectively prevented water molecules from diffusing through the PMGI layer, while still allowing penetration of hydrogen. The response time was defined as the time required to reach 90 % of peak current after 500 ppm hydrogen exposure, and recovery time as the time required to reach 10 % of the peak current after refreshing the device with dry air. The response times for the bare and PMGI diodes were 3 s and 4 s respectively, but the recovery times were 3 s and 251 s. To reduce the longer recovery time of the PMGI encapsulated Pt nanonetwork sensor, optimization of the thickness of PMGI layer and PMGI deposition method including post-annealing temperature, time, and ambient are required.

The polyimide based PMGI has excellent thermal stability, with a glass transition temperature of 335 °C [17]. The hydrogen response of the PMGI encapsulated Pt nanonetwork Schottky diode for both dry and wet hydrogen exposures was tested up to 300 °C on the heated chuck in the gas test chamber, as shown in Fig. 5. Repeated cycles of 500 ppm dry or humid hydrogen were infused into the device at 100 °C, 200 °C, and 300 °C in the test chamber. The operating bias voltages were chosen for the maximum responsivity at each temperature (1 V, 0.9 V, and 0.9 V for 100 °C, 200 °C, and 300 °C respectively). Reliable and stable current response to both dry and wet hydrogen was observed, with the shape of the Pt nanonetwork in PMGI encapsulation layer maintained up to 300 °C (Fig. 2).

Fig. 6 shows the responsivity of the bare and PMGI coated devices with Pt nanonetwork to 500 ppm dry hydrogen in the temperature range of 25 °C–300 °C. The responsivity is defined as $\frac{I_H - I_{air}}{I_{air}} \times 100\,\%$, where I_H is the current under 500 ppm hydrogen ambient and I_{air} is under air ambient. At 25 °C, the responsivities of uncoated and encapsulated sensors were 1.57×10^7 % and 5.79×10^7 %, respectively. The PMGI coated device showed a peak responsivity of 3.81×10^9 % at 150 °C and exhibited a decrease at high temperatures, while the responsivity of bare devices decreased with temperature. At 150 °C where the responsivity started to decrease, is well below the glass transition temperature of PMGI (335 °C), and the shape of Pt nanonetwork in PMGI layer is unchanged up to 300 °C (Fig. 2). The decease of the responsivity for PMGI encapsulated Pt nanonetwork sensor could be due to the instability of the hydrogen-induced dipole layer above 200 °C [17,22]. The responsivity of the encapsulated sensor was investigated as a function of hydrogen concentration over the range of 0.1–40000 ppm at 25 °C with a dissociative Langmuir isotherm model as shown in Fig. 7. The Langmuir isotherm model is as follows [16,23,24].

$$\text{Responsivity} = \frac{\alpha (K_{eq} \bullet C)^{\frac{1}{2}}}{1 + (K_{eq} \bullet C)^{\frac{1}{2}}} \quad (1)$$

where α is the proportionality constant, K_{eq} is the equilibrium constant of the hydrogen adsorption on Pt surface, and C is the concentration of hydrogen in ppm. It was assumed that the responsivity is proportional to the number of hydrogens bound to active sites of the Pt nanonetwork surface. The K_{eq} is 1.39×10^{-2} for the Pt nanonetwork with PMGI encapsulation. The power of $\frac{1}{2}$ in Eq. (1) clearly indicates the dissociation of hydrogen molecules adsorbed on Pt surface, and the dissociative Langmuir isotherm matches very well with the measured data. As presented in the inset of Fig. 7, the PMGI encapsulated sensor with large surface area Pt nanonetwork could detect as low as 0.1 ppm hydrogen at 25 °C. The hydrogen gas selectivity of the Pt nanonetwork sensor with a PGMI moisture barrier over other gases was also tested. The device shows excellent hydrogen selectivity over 100 % N_2, 0.05 % NO_2, 0.1 % CO, 10 % CO_2, 4 % CH_4, and 100 % O_2 at 25 °C, as shown in Fig. 8. The current signal for the other gases was nominal compared to 500 ppm hydrogen. The forward bias voltage of the diode was maintained at 1.3 V, and the other detection conditions were same as the detection conditions as used for the H_2. The concentrations of the other gases were chosen in the range of U.S. health exposure limits by National Institute for Occupational Safety and Health [25].

Table 1 shows a comparison of hydrogen detection limits, detection range, operating temperature, and responsivity for this study, along with graphene, nitride, and oxide sensing materials [25–35]. Note that the PMGI encapsulated AlGaN/GaN based Pt nanonetwork sensor shows excellent limit of hydrogen detection and wide range of detection concentration and operating temperature. The previously reported degradation effect of humidity on sensing characteristics [26,33,35] are absent in our encapsulated diodes, which exhibit the same current response to both dry and wet hydrogen over a wide range of operating temperatures.

4. Conclusion

For highly sensitive and reliable operation of hydrogen sensors in both dry and humid ambient, AlGaN/GaN based Pt nanonetwork Schottky diodes with a PMGI water-blocking layer were demonstrated. For the conformal encapsulation of Pt nanonetwork with PMGI, the APTES treatment was adopted before PMGI coating on the Pt surface.

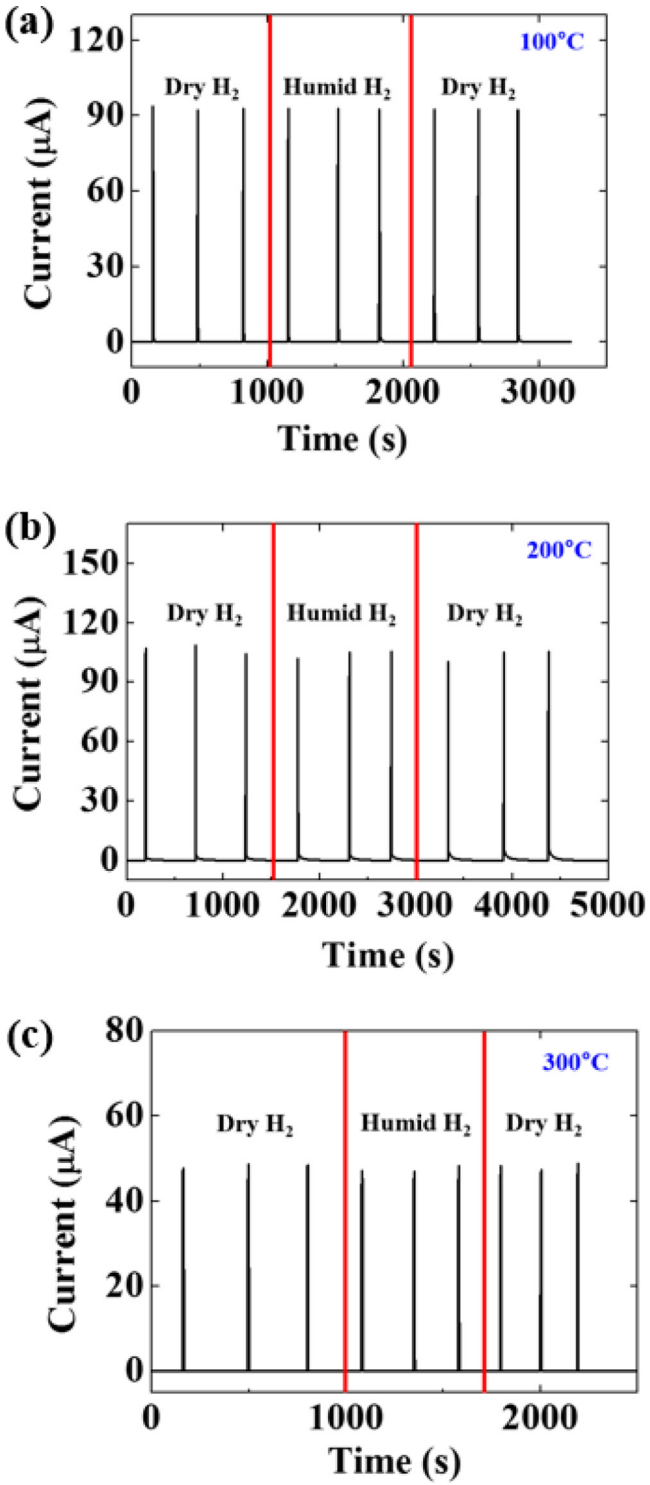

Fig. 5. Forward current response of the Pt nanonetwork diode with PMGI water-blocking layer for 500 ppm dry, humid, dry hydrogen exposures at (a) 100 °C and 1 V, 200 °C and 0.9 V, and 300 °C and 0.9 V.

The PMGI encapsulated device showed a high responsivity of 5.79×10^7 % and 3.81×10^9 % to 500 ppm hydrogen exposure at 25 °C and 150 °C respectively, and the limit of detection at 25 °C was 100 ppb. The PMGI coated sensor exhibited very stable operation up to 300 °C for both dry and wet hydrogen, with complete selectivity over other gases, including N_2, NO_2, CO, CO_2, CH_4, and O_2 at 25 °C. The PMGI encapsulation is a promising method to solve the humidity issue of semiconductor-based hydrogen sensors, signal drop in humid

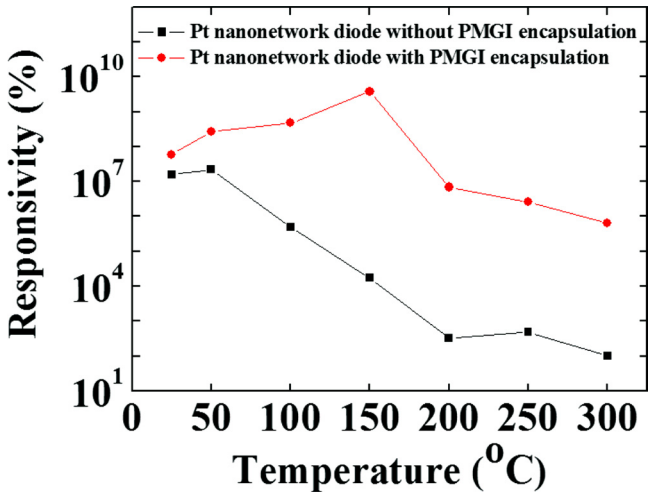

Fig. 6. H_2 responsivity of PMGI unencapsulated and encapsulated diodes upon 500 ppm dry hydrogen from 25 °C to 300 °C.

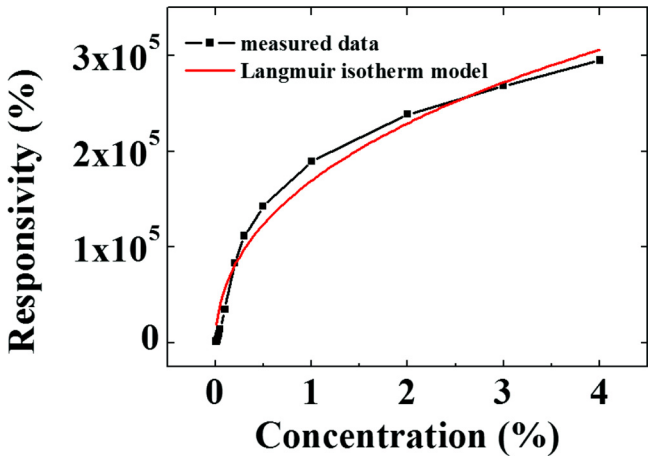

Fig. 7. Responsivity of the encapsulated sensor at 25 °C for a forward bias voltage of 1.3 V as a function of hydrogen concentration over the range of 0.1–4000 ppm with Langmuir isotherm model. The inset shows the current response of the diode for 0.1, 0.5, and 1 ppm H_2 exposure.

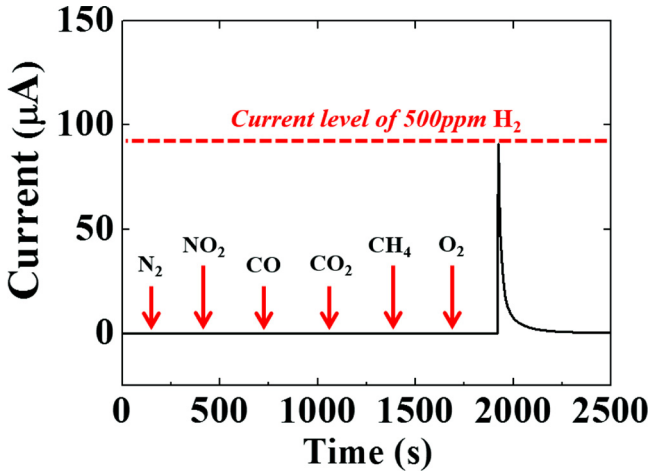

Fig. 8. Response of the PMGI encapsulated Pt nanonetwork sensor to sequential exposures of N_2 (100 %), NO_2 (0.05 %), CO (0.1 %), CO_2 (10 %), CH_4 (4 %), and O_2 (100 %) at 25 °C. The bias voltage was fixed at 1.3 V.

Table 1
Summary of hydrogen detection limits, detection range, operating temperatures, and responsivity for Pt nanonetwork on AlGaN/GaN in PMGI encapsulation, graphene, nitride and oxide-based materials [25–35].

	Substrate	Sensing material	Material Structure	Limit of detection (ppm)	Detection range (ppm)	Measurement temperature (°C)	Maximum responsivity (%)	Concentration used for responsivity (ppm)
This Study	Pt nanonetwoek	AlGaN/GaN	nanonetwork	0.1	0.1-40,000	25-300	3.8×10^{9}	500
Ref. [26]	Graphene oxide	SiO_2	nanosheet	100	100-1000	25	6.5	1000
Ref. [27]	Pd/TiO_2	SiO_2	nanotubes	1	10-5050	140-180	10^{5}	1000
Ref. [28]	Pd/SnO_2	SiO_2	film	500	500-10000	25	1.7×10^{4}	10000
Ref. [29]	Au/ZnO	Al_2O_3	film	75	75-1200	200-400	2.1×10	75
Ref. [30]	In_2O_3/graphene	SiO_2	nanocrystal	250	250-2000	250	9.5*	250
Ref. [31]	Pd/PANI/rGO	glass	film	100	100-20000	25-200	4.5×10	20000
Ref. [32]	SnO_2	Si	film	150	150-1000	25-125	1.9×10^{2}	1000
Ref. [33]	Pd/MoS_2	SiO_2	nanosheet	50	50-10000	25	3.5×10	10000
Ref. [34]	Pd	AlGaN/GaN	nanoparticle	50	50-10000	25-160	4.2×10^{8}	10000
Ref. [35]	GaN	Glass	nanoparticle	150	150-750	300-500	2.1×10^{3}*	750
Ref. [36]	Pd/HfO_2/GaO_X	AlGaN/GaN	film	5	5-1000	25-200	8.5×10^{9}	10000

* Responsivity has been re-calculated with the definition of $\frac{r_{ref}-r_{hydrogen}}{r_{ref}}\times100\%$ from the literature. The r_{ref} and $r_{hydrogen}$ are resistances in the reference and hydrogen gases respectively.

ambient, and will extend practical applications for GaN-based hydrogen sensors to temperatures up to ~300 °C.

Declaration of Competing Interest

The authors declare that they have no known competing financial interests or personal relationships that could have appeared to influence the work reported in this paper.

Acknowledgments

This research was supported by Basic Science Research Program through the National Research Foundation of Korea (NRF) funded by the Ministry of Education (2018R1D1A1A09083988, 2017R1D1A3B03035420), and Nano·Material Technology Development Program through the National Research Foundation of Korea (NRF) funded by the Ministry of Science, ICT and Future Planning (2015M3A7B7045185). The work at UF was supported by DTRA grant HDTRA1-17-1-0011

References

[1] MAN Company, Vorrichtung zur fortlaufenden Bestimmung des Wasserstoffgehaltes in Gasgemischen, Patent DRP 165 349 (1904).
[2] T. Hübert, L. Boon-Brett, G. Black, U. Banach, Hydrogen sensors-A review, Sens. Actuators B Chem. 157 (2011) 329–352.
[3] Z. Li, Z.J. Yao, A.A. Haidry, T. Plecenik, L.J. Xie, L.C. Sun, Q. Fatima, Resistive-type hydrogen gas sensor based on Ti O_2: a review, Int. J. Hydrogen Energy 43 (2018) 21114–21132.
[4] L. Boon-Brett, J. Bousek, G. Black, P. Moretto, P. Castello, T. Hübert, U. Banach, Identifying performance gaps in hydrogen safety sensor technology for automotive and stationary applications, Int. J. Hydrogen Energy 35 (2010) 373–384.
[5] Y.S.H. Najjar, Hydrogen safety: the road toward green technology, Int. J. Hydrogen Energy 38 (2013) 10716–10728.
[6] C. San Marchi, E.S. Hecht, I.W. Ekoto, K.M. Groth, C. LaFleur, B.P. Somerday, R. Mukundan, T. Rockward, J. Keller, C.W. James, Overview of the DOE hydrogen safety, codes and standards program, part 3: advances in research and development to enhance the scientific basis for hydrogen regulations, codes and standards, Int. J. Hydrogen Energy 42 (2017) 7263–7274.
[7] T. Hübert, L. Boon-Brett, V. Palmisano, M.A. Bader, Developments in gas sensor technology for hydrogen safety, Int. J. Hydrogen Energy 39 (2014) 20474–20483.
[8] S. Jang, S. Lee, K.H. Baik, Anisotropic electrical conductivity of surface-roughened semipolar GaN films by photochemical etching, J. Appl. Phys. 56 (2017) 051001.
[9] K.H. Baik, J. Kim, S. Jang, Highly sensitive nonpolar a-plane GaN based hydrogen diode sensor with textured active area using photo-chemical etching, Sens. Actuators B Chem. 238 (2017) 462–467.
[10] S. Jang, J. Kim, K.H. Baik, Enhanced hydrogen detection sensitivity of semipolar (11 $\bar{2}$ 2) GaN Schottky Diodes by surface wet etching on schottky contact, J. Electrochem. Soc. 163 (2016) B456–B459.
[11] S. Jang, P. Son, J. Kim, S. Lee, K.H. Baik, Hydrogen sensitive Schottky diode using semipolar (11 $\bar{2}$ 2) AlGaN/GaN heterostructures, Sens. Actuators B Chem. 222 (2016) 43–47.
[12] K.H. Baik, H. Kim, S. Lee, E. Lim, S.J. Pearton, F. Ren, S. Jang, Hydrogen sensing characteristics of semipolar (11 $\bar{2}$ 2) GaN Schottky diodes, Appl. Phys. Lett. 104 (2014) 072103.
[13] H. Kim, S. Jang, AlGaN/GaN HEMT based hydrogen sensor with platinum nanonetwork gate electrode, Curr. Appl. Phys. 13 (2013) 1746–1750.
[14] H. Kim, W. Lim, J. Lee, S.J. Pearton, F. Ren, S. Jang, Highly sensitive AlGaN/GaN diode-based hydrogen sensors using platinum nanonetworks, Sens. Actuators B Chem. 164 (2012) 64–68.
[15] S. Jang, S. Jung, K.H. Baik, Hydrogen sensing characteristics of Pt Schottky diode on nonpolar m-plane (11 $\bar{0}$0) GaN single crystals, Thin Solid Films 660 (2018) 646–650.
[16] K.H. Baik, S. Jung, F. Ren, S.J. Pearton, S. Jang, Moisture Insensitive PMMA Coated Pt-AlGaN/GaN Diode Hydrogen Sensor and Its Thermal Stability, ECS J. Solid State Sci. Technol. 7 (2018) Q3009–Q3013.
[17] S. Jung, K.H. Baik, F. Ren, S.J. Pearton, S. Jang, Temperature and humidity dependence of response of PMGI-Encapsulated Pt-AlGaN/GaN diodes for hydrogen sensing, IEEE Sens. J. 17 (2017) 5817–5822.
[18] S. Jung, K.H. Baik, F. Ren, S.J. Pearton, S. Jang, Pt-AlGaN/GaN hydrogen sensor with water-blocking PMMA layer, IEEE Electron Device Lett. 38 (2017) 657–660.
[19] Y. Song, R.M. Garcia, R.M. Dorin, H. Wang, Y. Qiu, E.N. Coker, W.A. Steen, J.E. Miller, J.A. Shelnutt, Synthesis of platinum nanowire networks using a soft template, Nano Lett. 7 (2007) 3650–3655.
[20] G. Guisbiers, G. Abudukelimu, D. Hourlier, Size-dependent catalytic and melting properties of platinum-palladium nanoparticles, Nanoscale Res. Lett. 6 (2011) 396.
[21] R.J. Ashley, Permeability and plastics packaging, in: J. Comyn (Ed.), Polymer Permeability, Springer, Dordrecht, 1985, pp. 269–308.
[22] B.H. Chu, C.F. Lo, J. Nicolosi, C.Y. Chang, V. Chen, W. Strupinski, S.J. Pearton, F. Ren, Hydrogen detection using platinum coated graphene grown on SiC, Sens. Actuators B Chem. 157 (2011) 500–503.
[23] C. Wen, Q. Ye, S. Zhang, D. Wu, Assessing kinetics of surface adsorption–desorption of gas molecules via electrical measurements, Sens. Actuators B Chem. 223 (2016) 791–798.
[24] G. Lee, S. Kim, S. Jung, S. Jang, J. Kim, Suspended black phosphorus nanosheet gas sensors, Sens. Actuators B Chem. 250 (2017) 569–573.
[25] NIOSH Pocket Guide to Chemical Hazards, (2020) https://www.cdc.gov/niosh/npg/default.html.
[26] J. Wang, B. Singh, J.H. Park, S. Rathi, I.Y. Lee, S. Maeng, H.I. Joh, C.H. Lee, G.H. Kim, Dielectrophoresis of graphene oxide nanostructures for hydrogen gas sensor at room temperature, Sens. Actuators B Chem. 194 (2014) 296–302.
[27] J. Moon, H.P. Hedman, M. Kemell, A. Tuominen, R. Punkkinen, Hydrogen sensor of Pd-decorated tubular TiO2 layer prepared by anodization with patterned electrodes on SiO2/Si substrate, Sens. Actuators B Chem. 222 (2016) 190–197.
[28] C. Ling, Q. Xue, Z. Han, H. Lu, F. Xia, Z. Yan, L. Deng, Room temperature hydrogen sensor with ultrahigh-responsive characteristics based on Pd/SnO2/SiO2/Si heterojunctions, Sens. Actuators B Chem. 227 (2016) 438–447.
[29] Q.A. Drmosh, Z.H. Yamani, Synthesis, characterization, and hydrogen gas sensing properties of AuNs-catalyzed ZnO sputtered thin films, Appl. Surf. Sci. 375 (2016) 57–64.
[30] M. Mansha, A. Qurashi, N. Ullah, F.O. Bakare, I. Khan, Z.H. Yamani, Synthesis of In2O3/graphene heterostructure and their hydrogen gas sensing properties, Ceram. Int. 42 (9) (2020) 11490–11495.
[31] Y. Zou, Q. Wang, C. Xiang, C. Tang, H. Chu, S. Qiu, E. Yan, F. Xu, L. Sun, Doping composite of polyaniline and reduced graphene oxide with palladium nanoparticles for room-temperature hydrogen-gas sensing, Int. J. Hydrogen Energy 41 (2016) 5396–5404.
[32] I.H. Kadhim, H.A. Hassan, Q.N. Abdullah, Hydrogen gas sensor based on nanocrystalline SnO 2 thin film grown on bare Si substrates, Nano-Micro Lett. 8 (2016) 20–28.
[33] D.H. Baek, J. Kim, MoS2 gas sensor functionalized by Pd for the detection of hydrogen, Sens. Actuators B Chem. 250 (2017) 686–691.
[34] H.I. Chen, Y.C. Cheng, C.H. Chang, W.C. Chen, I.P. Liu, K.W. Lin, W.C. Liu,

Hydrogen sensing performance of a Pd nanoparticle/Pd film/GaN-based diode, Sens. Actuators B Chem. 247 (2017) 514–519.
[35] A. Hermawan, Y. Asakura, M. Kobayashi, M. Kakihana, S. Yin, High temperature hydrogen gas sensing property of GaN prepared from α-GaOOH, Sens. Actuators B Chem. 276 (2018) 388–396.
[36] C.H. Chang, K.W. Lin, H.H. Lu, R.C. Liu, W.C. Liu, Hydrogen sensing performance of a Pd/HfO2/GaOx/GaN based metal-oxide-semiconductor type Schottky diode, Int. J. Hydrog. Energy. 43 (2018) 19816–19824.

Kwang Hyeon Baik received the B.S. degree at Yonsei University, Seoul, Koreain 1998, and Ph.D. degree in Materials Science and Engineering from University of Florida, Gainesville, Florida in 2004. He worked at the Photonics Lab at Sam-sung Advanced Institute of Technology from 2005 to 2008, and also worked at the Korea Electronics Technology Institute from 2009 to 2011. Since 2012, he has been with Hongik University, Sejong, Korea as an associate professor. His current research interests include the growth and characterization of GaN and ZnO-based light-emitting diodes and hydrogen gas sensors, and III–V semiconductor-based electronic devices.

Sunwoo Jung received his MS degree in the department of Chemical Engineering at Dankook University, South Korea in 2018. He obtained his B.S. in Chemical Engineering at Dankook University in 2016. His research has focused on nitride and oxide based chemical sensors.

Kyung-Ho Park received Ph. D. degree in Applied Physics from the Ajou University, Republic of Korea in 2002. He was a Post-Doctoral Researcher at the Department of Engineering of Cambridge University from 2002 to 2003. From 2003 to 2005, he was a research professor at Ajou University. In 2005, he joined Korea Advanced Nano Fab Center, where he is currently a general manager of device technology division. His current research interests include fabrication and characterization of GaN HEMT sensor, GaAs magnetic Hall sensor, and MEMS devices.

Chu-Young Cho received Ph. D. degree in 2011 from School of Materials Science and Engineering at Gwangju Institute of Science & Technology, South Korea. He was a Post-Doctoral Research Fellow at the Center for Quantum Devices in Northwestern University, before joining Korea Advanced Nano Fab Center (KANC), where he is currently a senior researcher of Nanodevice Laboratory. His major research focuses on the MOCVD growth of the GaN based semiconductors for highly efficient LEDs and electronic devices.

Fan Ren is Charles A. Stokes professor of Chemical Engineering at the University of Florida, Gainesville, FL, USA. Prior to joining UF in 1998, he worked for AT&T Bell Laboratories for 13 years as a Member of Technical Staff. His current research interests include semiconductor based sensors, Ga_2O_3 based power devices and nitride based HEMTs. He is a fellow of ECS, MRS, IEEE, SPIE, APS and AVS.

Stephen J. Pearton is a distinguished professor and Alumni Chair of Materials Science and Engineering at the University of Florida, Gainesville, FL, USA. He has Ph.D. in physics from the University of Tasmania and was a Post-Doc at UC Berkeley prior to working at AT&T Bell Laboratories in 1994–2004. His interests are in the electronic and optical properties of semiconductors. He is a fellow of the IEEE, AVS, ECS, MRS, SPIE, TMS and APS.

Soohwan Jang received the B.S. degree in Department of Chemical Engineering from Seoul National University, Seoul, Korea in 2003. He also received the Ph.D. degree in Department of Chemical Engineering from University of Florida, Gainesville, Florida in 2007. From 2007 to 2009, he worked in Samsung Electronics. He has been a professor at the Department of Chemical Engineering at Dankook University since 2009. His research interests include nitride and oxide based sensors, light emitting diodes, and integrated electronic devices.